

## Optimizing the carbonization temperature in the fabrication of waste cotton based activated carbon used as electrode material for supercapacitor

Nguyen K. Thach<sup>1,2,a</sup>, Ilya S. Krechetov<sup>1,b</sup>, Valentin V. Berestov<sup>1,c</sup>,  
Tatyana L. Lepkova<sup>1,d</sup>, Svetlana V. Stakhanova<sup>1,3,e</sup>

<sup>1</sup>National University of Science and Technology “MISIS”, Moscow, Russia

<sup>2</sup>Vietnam National University of Forestry, Hanoi, Vietnam

<sup>3</sup>Mendeleev University of Chemical Technology of Russia, Moscow, Russia

<sup>a</sup>[nguyenkienthach@gmail.com](mailto:nguyenkienthach@gmail.com), <sup>b</sup>[ilya.krechetov@misis.ru](mailto:ilya.krechetov@misis.ru), <sup>c</sup>[vberestov97@gmail.com](mailto:vberestov97@gmail.com),

<sup>d</sup>[lepkoval.tl@misis.ru](mailto:lepkoval.tl@misis.ru), <sup>e</sup>[stakhanova.s.v@muctr.ru](mailto:stakhanova.s.v@muctr.ru)

Corresponding author: N. K. Thach, [nguyenkienthach@gmail.com](mailto:nguyenkienthach@gmail.com)

**ABSTRACT** H<sub>3</sub>PO<sub>4</sub>-impregnated waste cotton was used as precursor to fabricate high porous activated carbon (AC) by the carbonization and activation processes with ultrahigh heating rate. The obtained activated carbon has unique physicochemical properties such as the structure mainly amorphous and ultrahigh specific surface area of 2769.7 m<sup>2</sup>/g for samples fabricated at carbonization temperature of 600 °C. The double-layer supercapacitors with activated carbon electrodes and electrolyte based on 1,1-dimethylpyrrolidinium tetrafluoroborate solution in acetonitrile of 1 M concentration were fabricated. The specific capacitance of electrode material fabricated from AC obtained at carbonization temperature of 600 °C reached 110.8 F/g at the current density of 50 mA/g and 85.1 F/g at 1000 mA/g. At 1000 mA/g, the degradation was less than 25% after 5000 charge/discharge cycles. The carbonization temperature of 600 °C is considered as optimum for fabricating activated carbon and the obtained activated carbon can be used for supercapacitor electrode materials.

**KEYWORDS** cotton, waste cotton, activated carbon, porous carbon, electrode material, supercapacitor, cellulose.

**FOR CITATION** Thach N.K., Krechetov I.S., Berestov V.V., Lepkova T.L., Stakhanova S.V. Optimizing the carbonization temperature in the fabrication of waste cotton based activated carbon used as electrode material for supercapacitor. *Nanosystems: Phys. Chem. Math.*, 2022, **13** (5), 565–573.

### 1. Introduction

Supercapacitors (SCs), also known as Electrochemical Capacitors, are devices that store electrical energy inside an electrical double layer (EDL) formed at the interface between the electrolyte solution and the solid-surface electrode with large surface area [1]. When compared to batteries, SCs have outstanding advantages such as high power density, large power conversion ratio, fast charge/discharge time, long life cycle, etc. While their disadvantage when compared in terms to batteries of the same mass and volume is their much lower energy density. Therefore, in commercial applications, SCs are often used in devices that support battery or fuel cell operation in the starting systems in which it is necessary to provide instantaneous electrical energy with high capacity for a short period of time such as automobiles, vehicles, trucks, buses, etc [2]. With the development of electronic technology in mobile devices, SCs are also used in intermittent energy recovery systems in automotive brake systems, solar cells, and small power electrical devices, etc.

The electrical energy capacity ( $E$ ) of an electrochemical double-layer supercapacitor (EDLS) is determined by  $E = \frac{1}{2}CV^2$ , where  $C$  is the capacitance of the capacitor and  $V$  is the operating voltage applied across the two electrodes. Consequently, operating voltage and capacitance are the two main factors affecting the energy storage capacity of EDLS. The operating voltage of SCs depend mainly on the electrolytes and solvents used. So, the electrolyte solutions need to have a large working potential window to maximize the electrical energy capacity. The aqueous electrolytes (acids, alkalis, inorganic salts) have a narrow potential window (0.8 – 1.2 V), making them unsuitable for commercial SCs. Moreover, during the capacitor's operation, the collectors are destroyed by the electrochemical corrosion that occurs on their surface, so the material used to make the current collectors must have high corrosion resistance such as stainless steel [3], silver, gold, etc. Therefore, it is expensive. However, the mobility and conductivity of ions in aqueous electrolytes are high and making them easy to use without strict storage conditions. In contrast to the aqueous electrolytes, organic electrolytes have large potential windows (2.5 – 3.5 V), and organic salts allow cheaper and less corrosive collector and enclosure materials. Recently, organic electrolyte solutions are increasingly used in commercial SCs.

Meanwhile, the capacitance of SCs depends on the surface area of the electrodes, the functional groups present on the surface, and the compatibility between the pore size distribution and the size of the electrolyte molecules. To increase the electrode surface area, materials with high porosity, specific surface area greater than  $1000 \text{ m}^2/\text{g}$ , have been commonly used in commercial SCs. With highly porous electrode materials, when the pore size is equivalent to the size of the electrolyte molecule, the interaction between the surface active sites and the electrolyte ions is quite weak and between the electrolyte–electrolytes dominate. Electrolyte–electrolyte interactions reduce the surface adsorption capacity for the electrolyte and thus lead to a decrease in the capacitance of the capacitor. If the pore size is too large compared to the electrolyte molecular size, the specific surface area of electrode is small, the density of surface active sites decreases, the electrolyte adsorption capacity decreases and leads to decrease capacitance of SCs.

In recent years, high porosity activated carbon from biomass has attracted much research attention of scientists, especially agricultural residues such as rice husk residue [4], sugarcane bagasse [5], cassava peel waste [6], cotton, cotton waste [7–10], etc. The activated carbon products meet the requirements for electrode materials such as large surface area, pore size that can be changed according to fabricating conditions and many surfaces functional groups. Moreover, these materials have many advantages such as low cost, availability, environment friendly and perfected electrode producing technology.

In our study, we focused on investigating the effect of carbonization temperature with ultrahigh heating rate on the properties of activated carbon obtained from  $\text{H}_3\text{PO}_4$ -impregnated waste cotton. First, the carbonization process conducted in argon atmosphere at various temperature from  $400 \text{ }^\circ\text{C}$  to  $800 \text{ }^\circ\text{C}$  with ultrahigh heating rate. Then, the physical activation process conducted in carbon dioxide atmosphere. By investigating the texture and electrochemical properties of obtained activated carbon, we propose the optimal carbonization temperature to produce activated carbon from waste cotton impregnated  $\text{H}_3\text{PO}_4$  used as electrode materials for supercapacitors.

## 2. Materials and methods

### 2.1. Preparation of activated carbon

*2.1.1. Impregnation of waste cotton.* Waste cotton was collected from Yartsevo Cotton Mill, LLC (Russia). 10 g of waste cotton was soaked in 300 g of 5 %  $\text{H}_3\text{PO}_4$  solution in a standard water bath. Then, the mixture was heated to a temperature range of  $80\text{--}85 \text{ }^\circ\text{C}$  and kept for 30 min. After the impregnation process, the cotton was squeezed out of water and dried at room temperature at least 24 h.

*2.1.2. Carbonization of waste cotton.* The carbonization was carried out in a horizontal furnace, the temperature and time controlled by Termodat controller. The carbonization temperatures were  $400 \text{ }^\circ\text{C}$ ,  $500 \text{ }^\circ\text{C}$ ,  $600 \text{ }^\circ\text{C}$ ,  $700 \text{ }^\circ\text{C}$  and  $800 \text{ }^\circ\text{C}$ . Initially, 4 g of shredded cotton was put into a quartz reactor chamber and supplied with a flow of Ar gas at a flow rate of 800 ml/min for 15 min to remove the air inside the reactor chamber. To achieve the ultrahigh heating rate for carbonization, the furnace was heated at a rate of  $10 \text{ }^\circ\text{C}/\text{min}$  until achieving the carbonization temperature. Then, the reactor chamber with cotton inside was put immediately into the furnace and maintained with a flow of Ar gas at a flow rate of 800 ml/min. The time of carbonization was 1 h. When the carbonization process finished, the reactor chamber was taken out, and cooled to the room temperature by the electric fan and the Ar flow at flow rate of 800 ml/min. The obtained products were weighed, and labeled with SP400, SP500, SP600, SP700, SP800 with carbonization temperatures of  $400 \text{ }^\circ\text{C}$ ,  $500 \text{ }^\circ\text{C}$ ,  $600 \text{ }^\circ\text{C}$ ,  $700 \text{ }^\circ\text{C}$  and  $800 \text{ }^\circ\text{C}$ , respectively.

*2.1.3. Activation.* All obtained products of carbonization are put into the reactor chamber. Ar gas with a flow rate of 800 ml/min was introduced into the reactor chamber for 15 minutes to remove air. The furnace first was heated to  $900 \text{ }^\circ\text{C}$  with the heating rate of  $10 \text{ }^\circ\text{C}/\text{min}$ . Then, the reactor chamber was put immediately into the furnace and maintained with a flow of Ar gas at a flow rate of 800 ml/min until reaches activation temperature of  $900 \text{ }^\circ\text{C}$ . Then, the Ar flow was interrupted, the  $\text{CO}_2$  flow was started and maintained at flow rate of 800 ml/min during the activation process. The activation time was 1 h. When activation process finished, the  $\text{CO}_2$  gas was interrupted, the Ar gas was started supplying at a flow rate of 800 ml/min. Then, the reactor chamber was taken out, and cooled to the room temperature by the electric fan and the Ar flow at flow rate of 800 ml/min. The activated carbon product was weighed and stored in a plastic bag to avoid dust and used for the next processes.

### 2.2. Physical characterization measurements of activated carbon

The surface morphology investigation of the activated carbon was performed on the focusing ion beam scanning electron microscope (SEM) TESCAN SOLARIS (Czech).

The investigation of specific surface area, pore volume, and pore size distribution was carried out by  $\text{N}_2$  adsorption-desorption isotherms at 77 K using a Gemini VII 2390 V1.02 (Micromeritics, USA).

The X-ray diffraction (XRD) spectra were conducted on an XPERT-PRO (Latvia).

TABLE 1. Minimum reactor chamber temperature, and heating rate of cotton carbonization

Samples	SP400	SP500	SP600	SP700	SP800
Minimum reactor chamber temperature, ( °C)	380 ± 10	471 ± 9	557 ± 13	638 ± 14	705 ± 7
Heating rate, ( °C/min)	321 ± 45	412 ± 44	466 ± 47	510 ± 62	577 ± 41

### 2.3. Preparation of supercapacitors and electrochemical measurements

Activated carbon was crushed with a mortar and mixed with polytetrafluoroethylene suspension F4D (Russia) as the binding material and carbon black (CABOT® VULCAN® XC72) as the electrically conductive component according to the mass ratio of 80:10:10, respectively. The mixture was placed in a glass flask containing 100 ml of 95 % alcohol (FEREIN, Russia) and stirred at room temperature for 30 minutes. The slurry was filtered through filter paper and rolled on a mechanical roller to form thin films with a thickness of 150  $\mu\text{m}$ . The thin films will then be cut into squares of different sizes for use as the capacitor's electrodes. The electrodes were dried at room temperature at least 24 h. Before use, the carbon electrodes were heated up to 120 °C for 2 h in the quartz tube with a flow rate of Ar of 100 ml/min and then weighed on a balance with an accuracy of 0.001 g.

The obtained carbon electrodes were pasted onto aluminum foils (OKURA-801, Japan) used as the collector of the supercapacitors by conductive adhesive (RIKON, Russia). The two complete electrodes are placed opposite each other and separated by a separator TF-40-30 (Japan). The electrode system was placed in an adhesive enclosure and kept under vacuum at 120 °C for 48 h. Next, the enclosure was filled with 1 ml of 1,1-dimethylpyrrolidinium tetrafluoroborate (DMP·BF<sub>4</sub>) solution of 1 M concentration in acetonitrile (AN) solvent and packed to form a complete capacitor.

The cycle voltammetry characteristics of the capacitors were measured using P20-X potentiostat (Elins, Russia).

The charge/discharge tests were performed by the method of galvanostatic charge-discharge using ASK2.5.10.8 HIT analyzer (Russia).

## 3. Results and discussion

### 3.1. Heating rate and carbon yield

Cotton is a highly porous natural material. When conducting pyrolysis of cotton in an inert gas environment, cotton begin to thermally decompose at 250 °C and the process is intense in the range of 310 – 350 °C [11]. The pyrolysis's products include CO, CO<sub>2</sub>, H<sub>2</sub>O, and cellulose derivatives in liquid and gaseous states. When the temperature reaches above 350 °C, the cellulose decrystallization occurs. Currently, most studies in the field of biomass materials are conducted with heating rates between 5 °C and 20 °C and the reactor chamber is placed inside the furnace from room temperature along with the heating process. Therefore, the time of the heating process is usually greater than 1 h, and part of the cotton will undergo slow thermal decomposition. The products of the decomposition process penetrate inside the cotton fiber structure to prevent evaporation, reduce the decomposition rate of cellulose, and reduce the porosity of the cotton, leading to a decrease in the porosity of the obtained carbon.

To avoid slow thermal decomposition of cotton, we reduced the heating time for cotton from room temperature to the cellulose decrystallization temperature region to about 1 minute by carbonization method as described above. After the reactor was placed in the furnace, the temperature of the system suddenly dropped to the minimum value. The system then was heated up again to the carbonization temperature by the heating controller. The minimum temperature of the furnace and the heating rate of each carbonization temperature are shown in Table 1. From the data of Table 1, the minimum temperature of the reactor chamber for all samples is greater than 350 °C, the region where the cellulose decrystallization occurs. Above the cellulose decrystallization temperature, the thermal decomposition of cellulose takes place intensely and produces many derivatives in the liquid, gas, and vapor states. At high temperature and high Ar flow rate of 800 ml/min, these derivatives partly evaporate quickly from the cotton fiber surface and partly penetrate the cellulose crystal, destroying the crystal structure causing micro-swelling within the microstructure of the cellulose crystal, and facilitating the porous structure development. As a result, there are many close or open cavities inside the cotton fiber.

The carbon and activated carbon yields obtained after carbonization and activation processes are shown in Fig. 1. The yield of carbon obtained after carbonization decreased from 39.5% to 23.8% when the carbonization temperature was increased from 400 to 800 °C. This is consistent with the studies of M. J. Antal, et al [12]. As the carbonation temperature increases, the heating rate also increases, the decomposition of cellulose becomes more intense, producing more volatile derivatives and thus reducing the amount of coal obtained [13]. In contrast, we found that the yield of activated carbon is low and does not vary much for the samples. We suggested that, at high gas flow rates, CO<sub>2</sub> did not have enough time to diffuse deep into the carbon black structure and so instead of opening and expanding the inner pore structure, CO<sub>2</sub> burned most of carbon during activation.

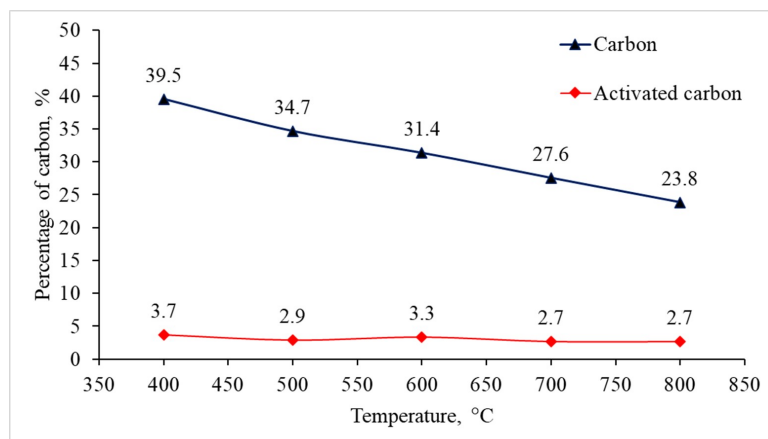


FIG. 1. Carbon yield after carbonization and activation of waste cotton at different carbonization temperatures

### 3.2. Physical properties

Figure 2 shows the X-ray diffraction (XRD) spectrum of the samples at different temperatures. The peak of graphite crystals (002) at  $2\theta \sim 25^\circ$  was low and no significant existence of graphite (001) at  $2\theta \sim 44^\circ$  was observed. This shows that the obtained activated carbon material has a structure mainly of amorphous carbon material.

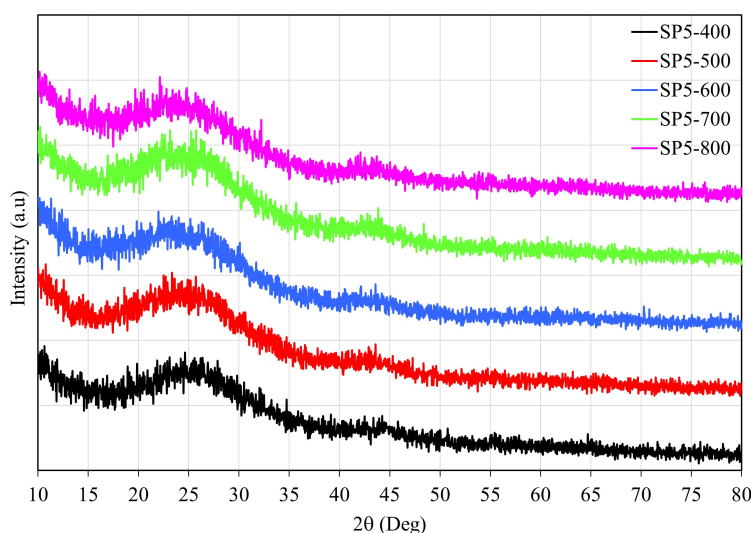


FIG. 2. X-ray diffraction spectrum of activated carbons prepared at different carbonization temperatures

Figure 3 shows the SEM image of the SP600 sample at different magnitudes. Fig. 3a shows that the activated carbon fiber surface is quite smooth, clear, and free of impurities adhering to the surface. Cotton fibers are characteristically flattened, twisted, and have an average diameter of less than  $10 \mu\text{m}$ . As in Fig. 3b, the surface structure of cotton fibers after activation retains the characteristic structure of cotton with many folds on the surface. At  $100 \text{ nm}$  magnitude (Fig. 3c), there are many small and uniform pore structures at the cotton fiber surface. This demonstrates that there has been a well-developed porous structure within the obtained activated carbon material. The size of the porous structures distributed in the region of micropores and mesopores.

The texture characteristics of activated carbon were identified by  $\text{N}_2$  adsorption-desorption measurement at  $77 \text{ K}$ . The Brunauer, Emmet, and Teller (BET) method and the Barrett, Joyner, and Halenda (BJH) method were used to determine the specific surface area and pore size distribution within the activated carbon. The  $\text{N}_2$  adsorption-desorption isotherms of the samples (Fig. 4) have the form corresponding to Type I(b) and Type II according to the IUPAC classification system [14, 15]. When the relative pressure  $p/p_0 < 0.99$ , the sorption isotherm has the form corresponding to Type I(b) with the pore structure distributed mainly in the micropores region and partly extended to the mesopores region with pore size less than  $2.5 \text{ nm}$ . These adsorption isotherms do not show the appearance of hysteresis loops for all samples. When the relative pressure  $p/p_0 = 1$ , there is an increasing without limit in the adsorption isotherms, corresponding to Type II with the appearance of macropores.

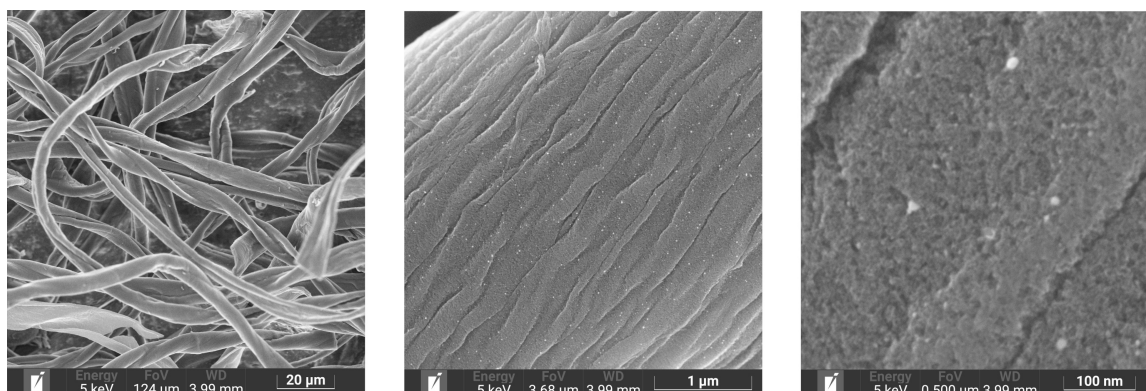


FIG. 3. SEM images of the sample SP600 at different magnitudes

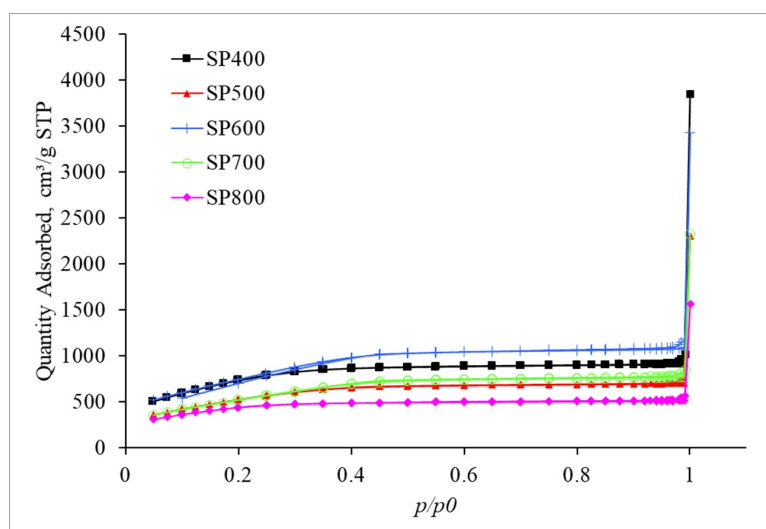


FIG. 4.  $N_2$  adsorption-desorption isotherms at 77 K of the samples prepared at different carbonization temperatures

Table 2 is the surface characteristic of activated carbon of all samples. The specific area ( $S_{BET}$ ) was calculated by BET method with relative pressure ( $p/p_0$ ) from 0.05 to 0.35. Total pore volume ( $V_{pore}$ ) and average pore size ( $d$ ) were calculated by BJH method. According to the data of Table 2, the specific surface area and total pore volume of the porous activated carbon samples reached the highest value for the sample SP600 with  $S_{BET} = 2769.7 \text{ m}^2/\text{g}$ ,  $V_{pore} = 2.09 \text{ cm}^3/\text{g}$  and the lowest value with sample SP800 with  $S_{BET} = 1433.4 \text{ m}^2/\text{g}$ ,  $V_{pore} = 0.74 \text{ cm}^3/\text{g}$ . When the carbonization temperature is less than  $600 \text{ }^\circ\text{C}$ , the specific surface area and total pore volume change randomly. Meanwhile, when the carbonization temperature is greater than  $600 \text{ }^\circ\text{C}$ , the specific surface area and total pore volume decrease as the carbonization temperature increases. This can be explained that at the carbonization temperature of  $400 \text{ }^\circ\text{C}$  and  $500 \text{ }^\circ\text{C}$ , the thermal decomposition of cellulose in cotton creates small-sized and partially sealed primary pores inside the cotton fiber structure. During activation,  $\text{CO}_2$  reacts with the carbon on the pore wall and partially opens these sealed hollow structures. Therefore, the specific surface area and total pore volume change unevenly with increasing temperature. But at the carbonization temperature of  $600 \text{ }^\circ\text{C}$ ,  $700 \text{ }^\circ\text{C}$ , and  $800 \text{ }^\circ\text{C}$ , the thermal decomposition takes place intensely and creates more open primary pore structures and larger sizes when increasing temperature. When activation takes place,  $\text{CO}_2$  removes carbon and further enlarges these pores and thereby reduces the specific surface area and total pores volume of the porous material. The BJH method is only applicable to determine the size of pores distributed in the mesopores and macropores regions. Therefore, the calculated average size of pores in Table 2 does not vary much for all samples and ranges from 2 – 3 nm.

Figure 5 shows the distribution of the pore sizes determined by the BJH method. It shows that all samples have a major peak in the micropores region and neighboring mesopores with size less than 2.5 nm and a minor peak in the macropores region with size larger than 50 nm. This is consistent with the characteristics of the nitrogen adsorption isotherms discussed above. Furthermore, as the carbonization temperature increases, there is an additional peak in the 4 – 5 nm region for SP700 and SP800 samples. This again demonstrates that as the carbonation temperature increases, the size of the primary pores inside the carbon black structure becomes larger, so there is a shift in pores size to a larger region.

TABLE 2. Surface characteristics of activated carbon of the SP400, P500, SP600, SP700, SP800 samples

Samples	$S_{BET}$ (m <sup>2</sup> /g)	$V_{pore}$ (cm <sup>3</sup> /g)	$d$ (Å)
SP400	2535.5	1.49	25.18
SP500	1883.7	1.47	27.67
SP600	2769.7	2.09	26.17
SP700	1931.0	1.53	27.90
SP800	1433.4	0.74	24.80

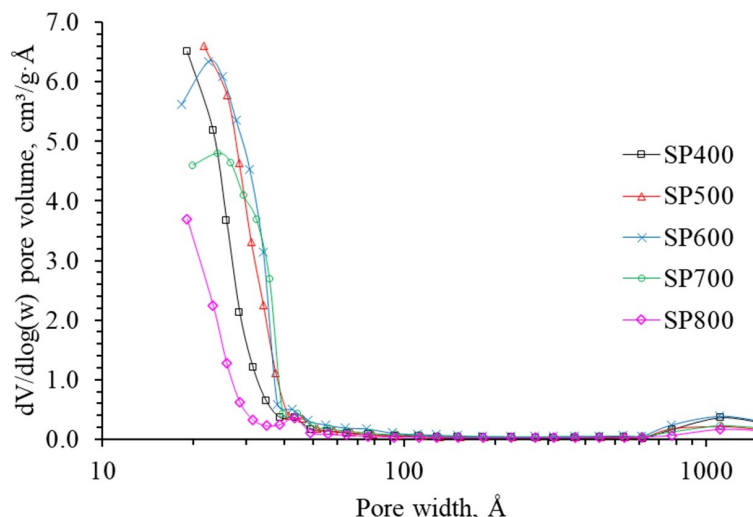


FIG. 5. The pore size distribution of the samples according to the BJH method

### 3.3. Electrochemical properties

Figure 6 shows the cyclic voltammogram (CV) curves with potential scan rates of 100 mV/s and the galvanostatic charge-discharge (GCD) curves at specific current density of 1000 mA/g for all samples. The change in shape of the CV curves is closely related to the equivalent series resistance (ESR) of the supercapacitor. The more like-rectangular the shape of the CV curves, the smaller the ESR and vice versa [16]. As shown in the Fig. 6a, the CV curves of the SP500, SP600, SP700 samples have the characteristic like-rectangular shape of an ideal capacitor and good reversibility but the samples SP400 and SP800 have not. This evidence shows that the electrochemical properties of the carbon electrode of the two samples SP400 and SP800 are worse than that of the other samples. Fig. 6b shows that the SP600 has the symmetric GCD curve, and the lowest voltage drop. The symmetry of the GCD curves reduces corresponding to the SP500, SP700 and finally SP400, and SP800. Again, the information from Fig. 6b shows that the SP600, and therefore the carbonization of the cotton at 600 °C, yielded activated carbon with the best electrochemical properties.

To assess the performance of fabricated capacitors, the specific capacitance of the capacitors was determined by the GCD method at specific density current from 50 mA/g to 5000 mA/g and presented at the diagram in Fig. 7. The SP600 capacitor achieved the highest specific capacitance from others with a value of 110.8 F/g at 50 mA/g and 85.1 F/g at 1000 mA/g. The value of the specific capacitance of the samples decreases as the specific current increases. However, Fig. 7 shows that there is a large difference between the change of the specific capacitance of the samples with increasing current density. Accordingly, the specific capacitance change of the SP600 capacitor is the smallest, followed by the SP700, SP500, and finally the SP400 and SP800 samples. The decrease in capacitance at high specific current densities is caused by the diffusion limitations of electrolyte ions inside the carbon electrodes [17].

One of the parameters affecting the performance of capacitors with organic electrolytes and organic solvents is their decomposition process when operating for a long time. The capacitors with AN solvent and ionic liquid electrolyte containing  $[BF_4]^-$  ion were studied in detail in our previous publish [18]. Accordingly, the carbon electrode fabrication process cannot completely remove the adsorbed water vapor inside the electrode material pores. The presence of water during the capacitor performance at high voltage causes water decomposition and leads to the decomposition of AN solvent and  $[BF_4]^-$  ions. The products of decomposition are usually a mixture of gases and precipitates. They diffuse into the porous structure, sealing the pores, thus preventing the adsorption of electrolyte solute molecules, reducing the

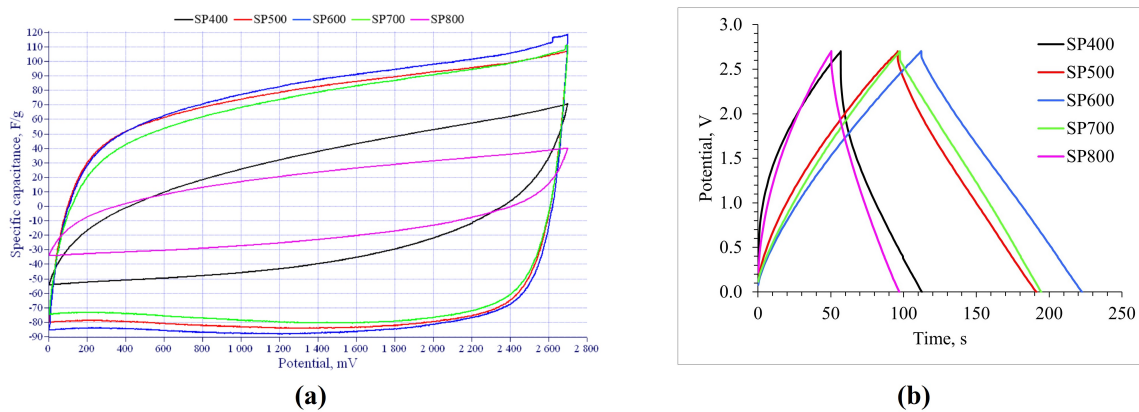


FIG. 6. (a) Cyclic voltammograms curves at potential scan rate of 100 mV/s and (b) galvanostatic charge-discharge curves at current density 1000 mA/g of the SCs with carbon electrodes fabricated at different carbonization temperatures

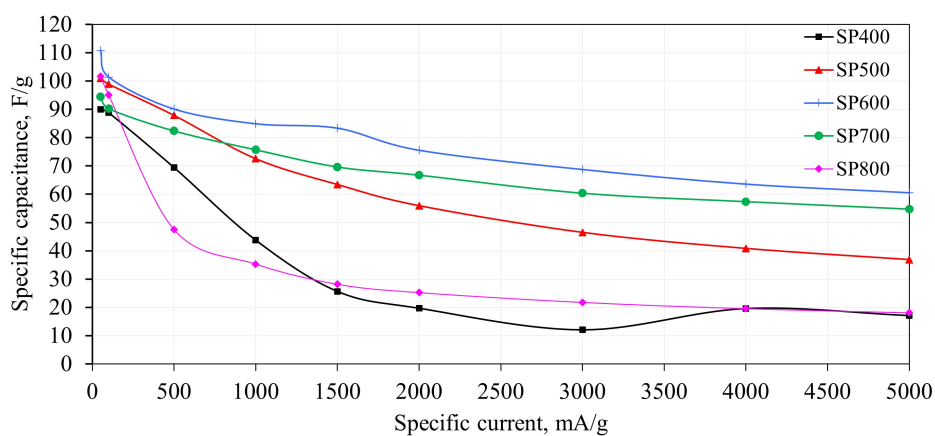


FIG. 7. Dependence of specific capacitance on the specific current densities of the capacitors

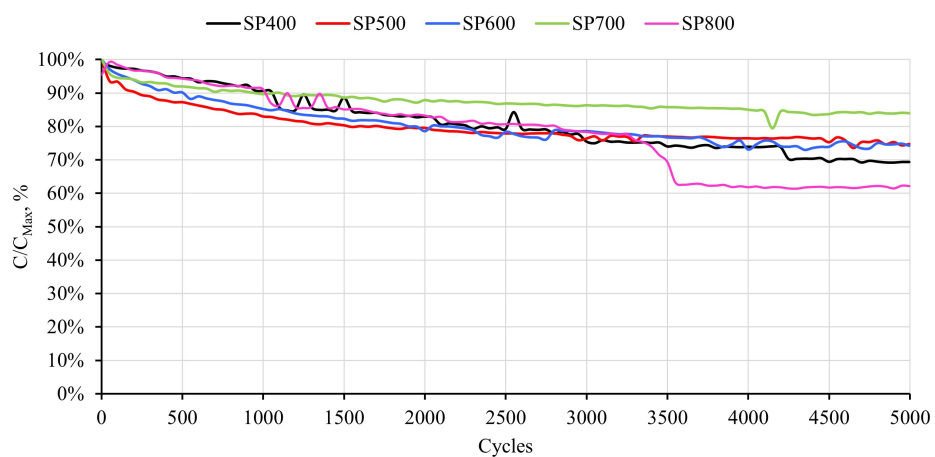


FIG. 8. Relative specific capacitance as a function of the charge-discharge cycles of the capacitors with 5000 cycles at a current density of 1000 mA/g

surface functional groups and specific surface area. The result is a decrease in the specific capacitance of the capacitor during operation.

The GCD method was used to investigate the life cycle of the capacitors. Fig. 8 shows the GCD curves of all capacitor samples with 5000 charge/discharge cycles at a specific current density of 1000 mA/g. The characteristic curve of the three samples SP500, SP600 and SP700 is quite smooth, and the relative specific capacitance decline is less than 25%, especially the SP700 sample, about 15%. This shows that the electrochemical properties of the carbon electrode as well as the electrode/collector junction of these capacitors are highly stable. On the opposite side, the relative specific capacitance curves of the SP400 and SP800 samples are unstable and have a sudden decline when the number of cycles reaches about 4200 and 3500 cycles, respectively. It shows that the electrochemical properties of the electrodes of the two samples are unstable.

#### 4. Conclusion

By the method of fast raising temperature of cotton carbonization above the cellulose decrystallization temperature in a short time with extra high heating rate, we have created activated carbon with unique physical and electrochemical properties. The ultrahigh specific surface area of ca. 2769.7 m<sup>2</sup>/g was obtained at carbonization temperature of 600 °C, with the pore size distribution mainly on the micropores region. There is a shift in pore size distribution from the micropores to the mesopores region with the increasing carbonization temperature. The capacitor with electrodes from activated carbon fabricated at the carbonation temperature of 600 °C exhibits better electrochemical properties and stable long-life cycles. Its specific capacitance values at current density 50 mA/g reached 110.8 F/g and the degradation of capacitance after 5000 cycles at 1000 mA/g less than 25 %. Therefore, the optimal temperature to obtain activated carbon with the best physicochemical properties for H<sub>3</sub>PO<sub>4</sub>-impregnated waste cotton is 600 °C and the obtained activated carbon can be fully satisfied used as electrode material for double layer supercapacitor.

#### References

- [1] Winter M., Brodd R.J. What are batteries, fuel cells, and supercapacitors? *Chemical Review*, 2004, **104**(10), P. 4245–4269.
- [2] Kö Tz R., Carlen M. Principles and Applications of Electrochemical Capacitors. *Electrochimica Acta*, 2000, **45**(15-16), P. 2483–2498.
- [3] Vijayakumar M., Santhosh R., Adduru J., Rao T.N., Karthik M. Activated carbon fibres as high performance supercapacitor electrodes with commercial level mass loading. *Carbon*, 2018, **140**, P. 465–476.
- [4] Luo Y., Li D., Chen Y., Sun X., Cao Q., Liu X. The performance of phosphoric acid in the preparation of activated carbon-containing phosphorus species from rice husk residue. *Journal of Materials Science*, 2019, **54**(6), P. 5008–5021.
- [5] Adib M.R.M., Suraya W.M.S.W., Rafidah H., Attahirah M.H.M.N., Hani M.S.N.Q., Adnan M.S. Effect of phosphoric acid concentration on the characteristics of sugarcane bagasse activated carbon. IOP Conf. Ser.: Mater. Sci. Eng. Langkawi, Malaysia, 27–29 October 2015, **136**(1), P. 012061.
- [6] Ismanto A.E., Wang S., Soetaredjo F.E., Ismadji S. Preparation of capacitor's electrode from cassava peel waste. *Bioresource Technology*, 2010, **101**(10), P. 3534–3540.
- [7] Sartova K., Omurzak E., Kambarova G., Dzhusmaev I., Borkoev B., Abdullaeva Z. Activated carbon, obtained from the cotton processing wastes. *Diamond and Related Materials*, 2019, **91**, P. 90–97.
- [8] Nahil M.A., Williams P.T. Pore characteristics of activated carbons from the phosphoric acid chemical activation of cotton stalks. *Biomass and Bioenergy*, 2012, **37**, P. 142–149.
- [9] Ma G., Guo D., Sun K., Peng H., Yang Q., Zhou X., Zhao X., Lei Z. Cotton-based porous activated carbon with a large specific surface area as an electrode material for high-performance supercapacitors. *RSC Advances*, 2015, **5**(79), P. 64704–64710.
- [10] Nahil M.A., Williams P.T. Characterisation of activated carbons with high surface area and variable porosity produced from agricultural cotton waste by chemical activation and co-activation. *Waste and Biomass Valorization*, 2012, **3**(2), P. 117–130.
- [11] Lewin M., Backer S., Hersh S.P., et al. *Cotton fiber chemistry and technology*. Phillip J. Wakelyn, Boca Raton, 2006, 176 p.
- [12] Antal M.J., Várhegyi G., Jakab E. Cellulose pyrolysis kinetics: Revisited. *Ind. Eng. Chem. Res.*, 1998, **37**(4), P. 1267–1275.
- [13] Brunner P.H., Roberts P.V. The significance of heating rate on char yield and char properties in the pyrolysis of cellulose. *Carbon*, 1980, **18**(3), P. 217–224.
- [14] Sing K.S.W., Everett D.H., Haul R.A.W., Moscou L., Pierotti R.A., Rouquérol J., Siemieniowska T. Reporting physisorption data for gas/solid systems-with special reference to the determination of surface area and porosity (Recommendations). *Pure and Applied Chemistry*, 1985, **57**(4), P. 603–619.
- [15] Thommes M., Kaneko K., Neimark A.V., Olivier J.P., Rodriguez-Reinoso F., Rouquerol J., Sing K.S.W. Physisorption of gases, with special reference to the evaluation of surface area and pore size distribution (IUPAC Technical Report). *Pure and Applied Chemistry*, 2015, **87**(9-10), P. 1051–1069.
- [16] Galimzyanov R.R., Stakhanova S.V., Krechetov I.S., Kalashnik A.T., Astakhov M.V., Lisitsin A.V., Rychagov A. Yu., Galimzyanov T.R., Tabarov F.S. Electrolyte mixture based on acetonitrile and ethyl acetate for a wide temperature range performance of the supercapacitors. *Journal of Power Sources*, 2021, **495**, P. 229442.
- [17] Tabarov F.S., Astakhov M.V., Kalashnik A.T., Klimont A.A., Krechetov I.S., Isaeva N.V. Micro-mesoporous carbon materials prepared from the hogweed (Heracleum) stalks as electrode materials for supercapacitors. *Russian Journal of Electrochemistry*, 2019, **55**(4), P. 265–271.
- [18] Kalashnik A.T., Galimzyanov R.R., Stakhanova S.V., et al. Degradation processes, leading to the generation of gas in a deep polarization of supercapacitors with organic electrolytes. *Rev. Adv. Mater. Sci.*, 2017, **50**, P. 62–68.

*Information about the authors:*

*Nguyen K. Thach*<sup>1,2,a</sup>, *Ilya S. Krechetov*<sup>1,b</sup>, *Valentin V. Berestov*<sup>1,c</sup>,

*Tatyana L. Lepkova*<sup>1,d</sup>, *Svetlana V. Stakhanova*. *K. Thach* – National University of Science and Technology “MISIS”, Leninskiy prospect 4, Moscow, 119049, Russia; College of electromechanical and civil engineering, Vietnam National University of Forestry, Hanoi, Vietnam; [nguyenkienthach@gmail.com](mailto:nguyenkienthach@gmail.com)

*Ilya S. Krechetov* – National University of Science and Technology “MISIS”, Leninskiy prospect 4, Moscow, 119049, Russia; [ilya.krechetov@misis.ru](mailto:ilya.krechetov@misis.ru)

*Valentin V. Berestov* – National University of Science and Technology “MISIS”, Leninskiy prospect 4, Moscow, 119049, Russia; [vberestov97@gmail.com](mailto:vberestov97@gmail.com)

*Tatyana L. Lepkova* – National University of Science and Technology “MISIS”, Leninskiy prospect 4, Moscow, 119049, Russia; [lepkova.tl@misis.ru](mailto:lepkova.tl@misis.ru)

*Svetlana V. Stakhanova* – National University of Science and Technology “MISIS”, Leninskiy prospect 4, Moscow, 119049, Russia; Mendeleev University of Chemical Technology of Russia, Miusskaya square 9, Moscow, 125047, Russia; [stakhanova.s.v@muctr.ru](mailto:stakhanova.s.v@muctr.ru)

*Conflict of interest:* the authors declare no conflict of interest.